Effect of Monovalent Ions on the Monolayers Phase Behavior of the Charged Lipid DPPG

D. Grigoriev,*,†,‡ R. Krustev,†,§ R. Miller,† and U. Pison||

Max-Planck Institut für Kolloid- und Grenzflächenforschung, Rudower Chaussee 5, D-12489 Berlin, Germany, St. Petersburg State University, Institute of Chemistry, Universitetskiy pr. 2, St.-Petersburg, 198904 Russia, Department of Physical Chemistry, University of Sofia, 1 J. Bourchier Ave., 1126 Sofia, Bulgaria, and Virchov-Klinikum, Augustenburger Platz 1, 13353 Berlin, Germany

Received: September 14, 1998; In Final Form: December 10, 1998

Brewster angle microscopy (BAM) studies on dipalmitoyl phosphatidyl glycerol (DPPG, sodium salt) monolayers on water subphases containing different amounts of NaCl are presented. Inhomogeneities in the monolayer appear after spreading at large mean areas per lipid molecule and at electrolyte concentrations in the subphase lower than 0.15 M NaCl. It is assumed that (i) after spreading DPPG is completely hydrolyzed, (ii) dissociation of the resulting acid depends on the electrolyte concentration in the subphase, and (iii) nondissociated acid molecules form solidlike aggregates in the monolayer, while the dissociated part surrounds them. Image processing of the BAM images allows us to calculate the surface densities of the lipid in the coexisting states, and the dissociation constant of the lipid in the monolayer (K_d^s). The electrostatic contribution to the surface pressure was estimated using the obtained K_d^s value. Comparison with the experimental π/A isotherms shows satisfactory agreement, confirming the value of the determined dissociation constant. We concluded that the described procedure is useful for the determination of K_d^s for monolayers of charged surfactant molecules.

Introduction

Research focusing on surfactants that resemble biological situations such as the alveoli lining layer in mammalian lungs has increased rapidly.[1−18] As model systems for such investigations, liposome dispersions[2−8] or monolayers of lipids on different aqueous subphases[3−5,7,9−18] are mainly used. Monolayers are physically preferable because they allow direct measurement of many system parameters that may characterize lipid layers in biological systems such as the lungs. In lungs, however, the lipid mixtures that cover the alveolar lining layer may exist in different forms: monolayers or multilayers. We conducted experiments with DPPG, one of the major components of lung surfactant.[2−18] This lipid is ionic and forms charged monolayers on an aqueous electrolyte subphase. The ionization state of DPPG depends on the electrolyte concentration in the subphase.[19,20] The ionization state can influence also the phase state of a monolayer and consequently its structure and properties. Therefore, investigations of DPPG monolayers on aqueous subphases containing different salt concentrations are interesting. Only very few papers, however, are dedicated to this topic.[21] It is unclear in what regard changes in the ionic content of the subphase alters phase behavior of the monolayer and determines the π/A isotherm shape.

Conventional Langmuir trough measurements combined with new optical methods, such as Brewster angle microscopy (BAM)[22] or fluorescence microscopy[23] yield new insights into the structure and properties of monolayers. In the present work Langmuir trough experiments combined with BAM aim at clarifying the state of DPPG monolayers as a function of salt concentration in the subphase. In addition, such insights should help to understand more clearly the pulmonary surfactant function.

Experiment

The measurements of the π/A isotherms were carried out on a PTFE Langmuir trough with a total area of about 260 cm^2. As a force detector, an electronic microbalance equipped with a Wilhelmy plate was used. Spreading of the lipid was performed from a stock 10^{-3} M DPPG solution in methanol/chloroform (1/3, v/v). Isotherms were recorded about 15 min after spreading to allow good solvent evaporation and equilibration of the monolayer with the subphase. The monolayers were compressed asymmetrically by one barrier at a constant speed of 1.19×10^{-3} nm^2 molecule^{-1} s^{-1}. Compression started at a mean area per molecule of about 1.2 nm^2 as an initial point. At least five isotherms were measured for each electrolyte subphase concentration to reach appropriate reproducibility.

The purity of the subphase surface was controlled by surface tension measurements during compression of an uncovered subphase. In all cases the surface pressure obtained in these blank tests was less than 0.1 mN/m, i.e., on the order of experimental accuracy. BAM studies were performed to visualize possible impurities as well. All measurements were performed at 20 ± 0.2 °C.

The Langmuir trough was positioned in the multiscope apparatus (OPTREL GmbH, Dr. Motschmann, Germany). It allows BAM video recording simultaneously with monolayer compression. Single digital BAM images were taken via a frame grabber and a suitable image processing program every 5 s. This time interval is necessary in order to observe completely new parts of the monolayer surface, which are moving because of the lateral flow caused by the barrier movement. BAM images

* Corresponding author.
† Max-Planck Institut für Kolloid- und Grenzflächenforschung.
‡ St. Petersburg State University.
§ University of Sofia.
|| Humboldt University.

10.1021/jp983704s CCC: $18.00
Published on Web 01/26/1999

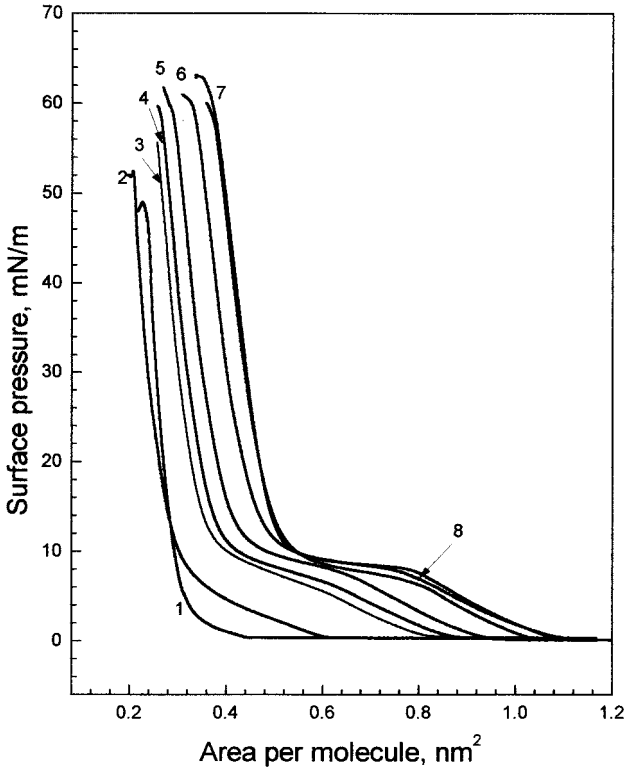

Figure 1. Compression isotherm π/A of DPPG spread on subphases containing different amounts of NaCl: (1) pure water; (2) 0.001 M; (3) 0.006 M; (4) 0.01 M; (5) 0.02 M; (6) 0.03 M; (7) 0.15 M; (8) 0.5 M. Temperature is 20 °C.

were transferred into binary (black/white) format and processed using conventional image analyzing software. The normalized numbers of pixels representing the respective monolayer phases were determined.

Dipalmitoyl phosphatidyl glycerol sodium salt was purchased from SIGMA and used without further purification. Methanol (Sigma) and chloroform (Fluka) were both spectroscopic grade and also used as obtained. Sodium chloride (Riedel-de Haen) was p.a. grade and recrystallized and heated at 600 °C to remove surface-active contaminations before use. Milli-Q deionized water (specific electrical conductivity of 18.2 MΩ cm) was used for the subphase preparation. The pH of the subphase was controlled periodically and was about 6.2.

Results and Discussion

The compression isotherms of DPPG spread on subphases at different NaCl concentrations are presented in Figure 1. Some important qualitative features can be considered from these isotherms. The plateau region of the isotherms became less pronounced with decreasing NaCl concentration. In addition, the kink point at which the plateau starts to appear is shifted to smaller surface pressures and mean molecular areas. The plateau completely disappears at the lowest electrolyte concentrations. A similar dependence of the isotherm shapes on the subphase electrolyte concentration and pH was observed earlier by Sacre and Tocanne.[21] Their assumptions, however, were based on the shape of the compression isotherms only without any information on the structure of the monolayers.

The trends in the behavior of isotherms are similar to the temperature dependencies for normal fatty alcohols and acids described earlier.[24] Such a tendency with decreasing temperature is normally associated with an increasing monolayer inhomogeneity. Recorded BAM images show that such inhomogeneities

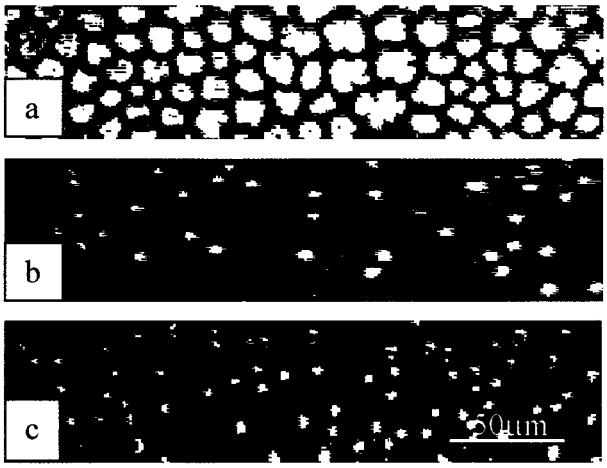

Figure 2. Typical BAM images taken at a mean area per DPPG molecule of 0.75 nm^2 and at different NaCl concentrations in the subphase: (a) 0.001 M; (b) 0.01 M; (c) 0.03 M

also exist in DPPG monolayers. Typical BAM pictures for the studied salt concentrations are presented in Figure 2. These pictures show that with decreasing NaCl concentration the average number of aggregates on the surface increases and their shape is more irregular. These aggregates appear immediately after spreading onto a solution of salt concentrations of 0.03 M NaCl, and they are stable during subsequent compression. Moreover, the appearance of aggregates can be observed even at a mean area per molecule of 35 nm^2. The above-mentioned tendencies in the shape of the isotherms cannot be explained only in terms of electrolytic dissociation of the ionic DPPG with a further increase of the electrostatic contribution to the surface pressure. Such behavior could be considered based on at least three different assumptions.

First, we assume that immediately after spreading, the whole quantity of DPPG is hydrolyzed into the respective acid (DPPGH).

$$\mathrm{DPPG^-} + \mathrm{HOH} \rightleftharpoons \mathrm{DPPGH} + \mathrm{OH^-} \qquad \text{(I)}$$

This acid is partly dissociated:

$$\mathrm{DPPGH} \leftrightarrow \mathrm{DPPG^-} + \mathrm{H^+} \qquad \text{(II)}$$

The dissociation constant K_d^s and the degree of dissociation α^s of this process are

$$K_d^s = \frac{[\mathrm{DPPG^-}]^s[\mathrm{H}]^s}{[\mathrm{DPPGH}]^s} \qquad (1)$$

$$\alpha^s = \frac{[\mathrm{DPPG^-}]^s}{[\mathrm{DPPGH}]^s + [\mathrm{DPPG^-}]^s} \qquad (2)$$

where the terms in brackets are equilibrium concentrations of each chemical species. The superscript s denotes that the equilibrium takes place in the surface layer.

Second, we assume that the degree of dissociation of the acid depends on the electrolyte concentration in the subphase. The higher the electrolyte concentration the higher is the degree of dissociation because protons are repelled by the increasing number of Na^+ ions in the diffuse double layer. Such behavior of lipid acids in monolayers was clarified in detail earlier.[19,20]

Third, we assume that at high mean areas per molecule all nondissociated DPPGH molecules are involved in the formation of monolayer aggregates. Dissociated molecules are regularly

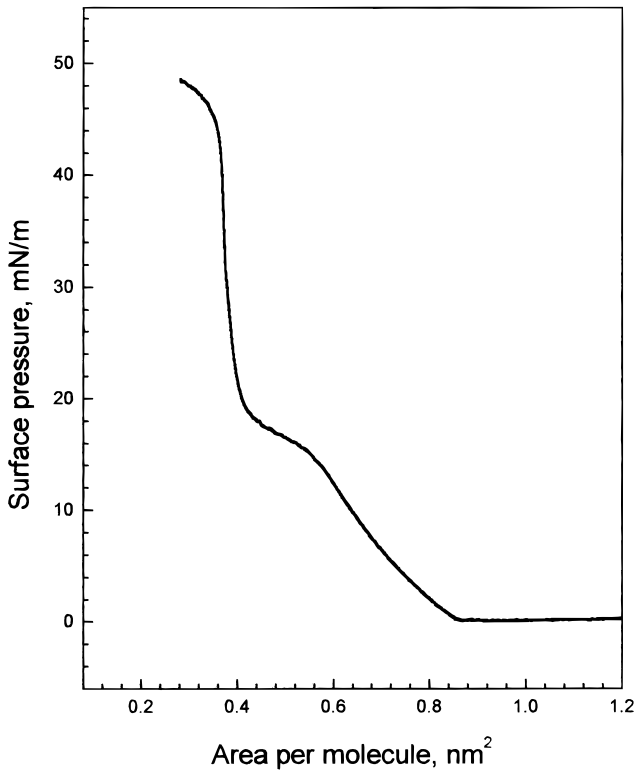

Figure 3. Compression isotherm π/A of DPPG spread on pure water at 40 °C.

distributed in the surface surrounding these aggregates. Hydrophobic interactions between alkyl chains of the lipid molecules are the driving forces for such aggregation. Hydrophobic interactions are supported by a relatively small hydrophilic headgroup, which allows the alkyl chains to come closer even at relatively high temperatures. Such behavior does not take place for instance in DPPC monolayers having equal hydrophobic chains but a larger headgroup. This third assumption was proved by obtaining a compression isotherm of DPPG on a pure water subphase but at a temperature of 40 °C. Under these conditions the entropy factor in the free energy of the aggregate formation process prevails over the enthalpy one, and no aggregates immediately after spreading should appear. The corresponding isotherm is presented in Figure 3 and supports the energetic nature of such aggregation.

These three assumptions and the obtained BAM images allow us to determine the degree of aggregation of the lipid (β), the dissociation constant of the lipid in the surface monolayer (K_d^s), and the electrostatic contribution to the surface pressure (π_{el}).

The degree of aggregation of the lipid is the ratio of the number of molecules involved in the formation of aggregates to the total number of spread molecules:

$$\beta \equiv \frac{N_{agg}}{N_{tot}} = \frac{N_A \Gamma_{agg} S_{agg}}{N_A[\Gamma_{agg} S_{agg} + \Gamma_{mon}(S - S_{agg})]} = \frac{\Gamma_{agg} S_{agg}}{\Gamma_{agg} S_{agg} + \Gamma_{mon}(S - S_{agg})} \quad (3)$$

where N_{agg} and N_{tot} are the number of molecules in the aggregates and the total number of spread molecules, N_A is Avogadro's number, Γ_{agg} and Γ_{mon} are surface densities of molecules in the monolayer aggregates and around them, respectively, S_{agg} is the area covered by aggregates, and S is the total area of the monolayer. If immediately after spreading aggregates consist only of the undissociated molecules, the degree of dissociation of DPPGH α^s on the surface can be determined as

$$\alpha^s = 1 - \beta \quad (4)$$

The two quantities Γ_{agg} and Γ_{mon} on the right-hand side of eq 3 can be calculated from the mass balance condition for the entire monolayer:

$$N_{tot} = N_A(\Gamma_{agg} S_{agg} + \Gamma_{mon}(S - S_{agg})) \quad (5)$$

$$\frac{N_{tot}}{N_A S} = \Gamma_{agg} \frac{S_{agg}}{S} + \Gamma_{mon} \frac{S - S_{agg}}{S} \quad (6)$$

Taking into account the mean area per molecule $A = S/N_{tot}$, we can rearrange eq 6 to

$$(AN_A)^{-1} = \frac{S_{agg}}{S}(\Gamma_{agg} - \Gamma_{mon}) + \Gamma_{mon} \quad (7)$$

Equation 7 represents a linear dependence in the coordinates $(AN_A)^{-1}$ vs (S_{agg}/S). The values of (S_{agg}/S) can be obtained directly from the BAM images as the ratio of the number of white pixels (representing the area occupied by aggregates) to the total pixel number of the image. Therefore, it is possible to calculate Γ_{agg} and Γ_{mon} using eq 7.

It must be noted that eq 7 can be applied only when in the whole plateau region Γ_{agg} and Γ_{mon} are not functions of the mean area per molecule A and the growth of the condensed phase is not related to changes in the structure of the aggregates. Such a condition is not fulfilled in reality, especially not at the lowest mean areas of this region; however, it can be accepted as a first approximation. One can also obtain a linear dependence of β on the mean area per molecule using eq 3 and the above-discussed condition about the independence of Γ_{agg} and Γ_{mon} on A:

$$\beta = N_A \frac{\Gamma_{agg}\Gamma_{mon}}{\Gamma_{mon} - \Gamma_{agg}} A - \frac{\Gamma_{agg}}{\Gamma_{mon} - \Gamma_{agg}} \quad (8)$$

A similar linear dependence of the degree of aggregation as a function of the mean area per molecule was obtained in ref 25. The authors used the assumption that the area per molecule in the monomer state in the whole plateau region is equal to the mean area per molecule at the onset of the LE−LC phase transition determined from the π/A isotherm as a kink point. Their consideration coincides with our assumption that Γ_{agg} and Γ_{mon} are not functions of A in the plateau.

The calculated results using the procedure described above are illustrated in Figure 4. Two different dependencies were found corresponding to a monolayer spread on a subphase containing 0.15 and 0.03 M NaCl, respectively. The first dependence for a subphase containing 0.15 M NaCl can be fitted by only one straight line. According to eq 7, its intercept represents the surface density in the monomer phase Γ_{mon}, while the slope is the difference $(\Gamma_{agg} - \Gamma_{mon})$. Here, the subscript *agg* corresponds to domains that appear in the process of compression. The second dependence for a subphase with a concentration of 0.03 M NaCl consists of two linear regions. The slope and intercept in the region of low S_{agg}/S values (region A) are related to aggregates appearing immediately after spreading and are different from usual domains. At higher S_{agg}/S values (region B) the obtained parameters Γ_{agg} and Γ_{mon} are in

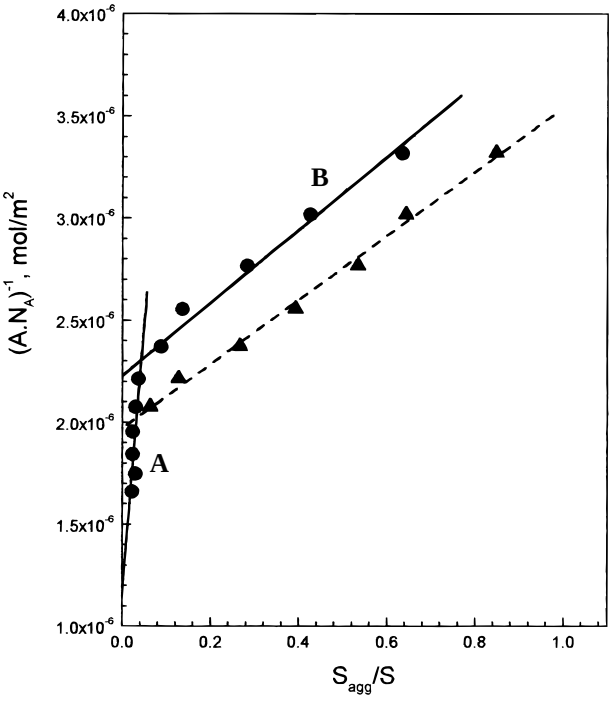

Figure 4. Dependencies $(AN_A)^{-1} = f(S_{agg}/S)$ calculated according to eq 7 for two NaCl concentrations in the subphase: (●) 0.03 M; (▲) 0.15 M. See text for details of the calculation procedure.

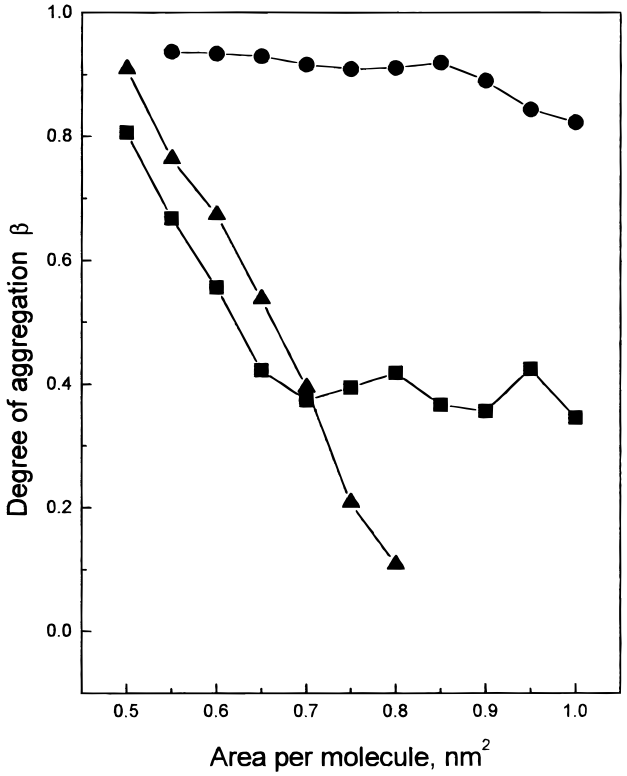

Figure 5. Dependence of the degree of aggregation β in DPPG monolayers on the mean area per molecule at different NaCl concentrations in the subphase: (●) 0.001 M; (■) 0.03 M; (▲) 0.15 M.

accordance with the surface density of that part of the aggregates that grow from the already existing nuclei during further monolayer compression. Therefore, this calculation procedure for intermediate NaCl concentrations yields two different sets of parameters Γ_{agg} and Γ_{mon}. Knowing Γ_{agg} and Γ_{mon} for each type of species allows us to obtain the degree of aggregation β using eq 3.

Some dependencies of the degree of aggregation on the mean area per molecule, $\beta = \beta(A)$, for different NaCl concentrations in the subphase are presented in Figure 5. At 0.001 M NaCl a large number of aggregates appear just after spreading. Thus, the degree of aggregation is high and varies only little upon subsequent compression. At 0.15 M NaCl aggregates appear with compression at the onset of the plateau region. Both curves can be calculated using only one set of parameters Γ_{agg} and Γ_{mon} for the nuclei of domains and normal domains, respectively. At 0.03 M NaCl aggregates behave differently. This curve was interpreted using two sets of data for Γ_{agg} and Γ_{mon}. Each of them represents a different stage of the evolution of domains in the monolayer. In this case eq 3 is not more valid for the whole molecular area range because it contains only one set of parameters Γ_{agg} and Γ_{mon}. Therefore, the calculation of β should be carried out step by step. In the region A the first set of parameters must be used. For the same procedure in the region B the Γ_{agg} values from both sets should be used but only one for Γ_{mon} corresponding to the homogeneous phase around the domains.

As mentioned above the β is directly related to the degree of dissociation α^s of DPPGH in the monolayer (eq 4) only for the nucleation region and electrolyte concentrations at which the inhomogeneity in the monolayer appears immediately after spreading.

In addition to β we determined the dissociation constant of the lipid in the surface monolayer (K_d^s). The degree of dissociation and the corresponding dissociation constant K_d^s are defined by eqs 1 and 2 and are not independent of each other. Both are functions of the proton concentration in the monolayer $[H^+]^s$, which can be determined following the approach in refs 19 and 20, which assumes that the distribution of the protons in the diffuse part of the electric double layer is described by the Boltzmann law:

$$[H^+]^s = [H^+] \exp\left(\frac{-e\psi_0}{kT}\right) \tag{9}$$

Here $[H^+]$ is the proton concentration in the bulk, e is the elementary charge, k is the Boltzmann constant, T is absolute temperature, and ψ_0 is electrical surface potential.

The ψ_0 was calculated using two independent equations for the surface charge density σ. One is the equation of Graham,

$$\sigma^2 = 2\epsilon\epsilon_0 kT\left(\sum_i \rho_{0i} - \sum_i \rho_{\infty i}\right) \tag{10}$$

where ϵ is the dielectric constant of the subphase, ϵ_0 is the vacuum permittivity, and ρ_{0i} is defined by the equation

$$\rho_{0i} = \rho_{\infty i} \exp\left(\frac{-z_i e\psi_0}{kT}\right) \tag{11}$$

$\rho_{\infty i}$ is the ionic concentration of ions i in the bulk, and $\pm z_i$ is the valence of these ions.

The other equation for calculating the electrical surface potential results from the insolubility of the $DPPG^-$ anions in the subphase:

$$\sigma = \frac{e}{A}\alpha^s \tag{12}$$

The square root of the right-hand side of eq 10 and the right-hand side of eq 12 are equal according to the electroneutrality of the whole system, and this allows us to determine ψ_0. Substituting ψ_0 into eq 9 and using the system of eqs 1 and 2

yields the value of the dissociation constant K_d^s of the dissociation process II.

The determination of K_d^s was performed only for some NaCl concentrations. The lowest electrolyte concentrations (0.001 and 0.006 M NaCl) were not used because of the extreme inhomogeneity, which can cause large errors in the determined S_{agg}/S values and hence in K_d^s. The highest concentrations (0.15 and 0.5 M NaCl) were also not taken into consideration because under these conditions the monolayer is homogeneous and no aggregates appear immediately after spreading.

The mean value of the equilibrium surface dissociation constant at three NaCl concentrations was calculated for mean areas per molecule at 1.0 nm^2 up to the onset of region B in steps of 0.05 nm^2. We obtained a K_d^s of 0.3 ± 0.2 mol/m^3 (pK_a = 3.52). The mean value of the constant is independent of the concentration of Na^+ in the suphase and the mean area per surfactant molecule within the limits of experimental errors. This is in accordance with the definition of the constant, which must not depend on these parameters. Sacre and co-workers obtained a comparable value for this constant (pK_a = 4.7).[21] These authors used a more complicated two-stage model[26] for the dissociation/association processes taking place at the surface. Perhaps this is the reason for the difference between their values and ours. Their model leads also to a dependence of the surface dissociation constant on the mean area per molecule in the monolayer and the subphase composition.

The electrostatic contribution to the surface pressure was calculated using the obtained K_d^s value. The approach developed in ref 19 has been used. The electrostatic contribution to the energy per molecule is calculated as

$$G_{el} = kT \ln(1 - \alpha^s) - \left(\frac{kT}{e}\right)^2 \kappa\epsilon\epsilon_0 A\left[\cosh\left(-\frac{e\psi_0}{2kT}\right) - 1\right] \quad (13)$$

where κ is the inverse Debye length for 1:1 electrolytes and described as

$$\kappa = \left(\frac{2e^2 N_A}{\epsilon\epsilon_0 kT} C_b\right) \quad (14)$$

Here, C_b is the sum of cation concentrations in the bulk phase.

The electrostatic contribution to the surface pressure π_{el}

$$\pi_{el} = -\frac{\partial G_{el}}{\partial A} \quad (15)$$

can be evaluated at different A and [Na^+] according to the relations 13−15 and knowing $\alpha^s(A,[Na^+])$ and $\psi_0(A,[Na^+])$. These two functions are interconnected by eqs 10−12. The first of them can be expressed by substitution of σ defined in eq 12 into eq 10 and solving the resulting expression according to α^s. The following application of eqs 1, 2, and 9 allows us to rearrange the resulting relationship into a form containing the other two unknown parameters—ψ_0 and K_d^s. Such a relationship gives the possibility of reducing errors in the determination of α^s by means of BAM image processing. Substitution of the mean K_d^s value yields the function $\psi_0 = \psi_0(A,[Na^+])$ (Figure 6a) and consequently $\alpha^s = \alpha^s(\psi_0(A,[Na^+]))$ or connected to this quantity through eq 12 function $\sigma = \sigma(A,[Na^+])$ (Figure 6b). In this way the electrostatic contribution to the surface pressure can be calculated.

The dependence of π_{el} and the experimental surface pressure π as a function of the subphase NaCl concentration in the subphase at a mean area per monolayer molecule of 0.85 nm^2 are presented in Figure 7. Both curves agree with each other. This shows that the obtained K_d^s value is reasonable. Similar dependencies are reported in ref 19. These experimental and calculated results agree better; however, the K_d^s values used by the authors are acceptable but not obtained experimentally. The substance for which such a comparison in ref 19 was fulfilled differs from ours in the alkyl chains length by four CH_2 groups. For that reason the assumed K_d^s must be in general higher than ours. However, the difference of some orders of magnitude is too large. Moreover, the agreement between our K_d^s and that in ref 21 shows that the value used in ref 19 was not well adjusted.

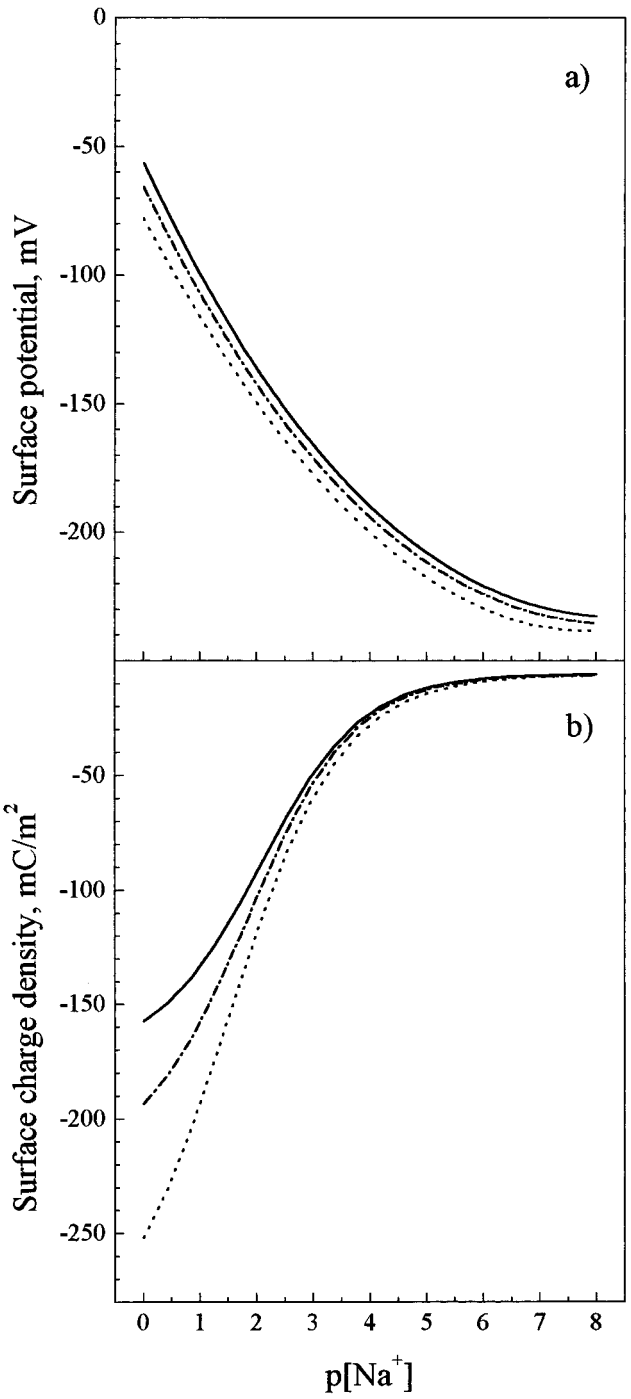

Figure 6. Dependencies of the surface potential (ψ_0) and the surface charge density (σ) on the Na^+ concentration in the subphase calculated according to eqs 10−12 at different areas per molecule: (straight line) 1.0 nm^2; (dot−dashed line) 0.8 nm^2; (dotted line) 0.6 nm^2.

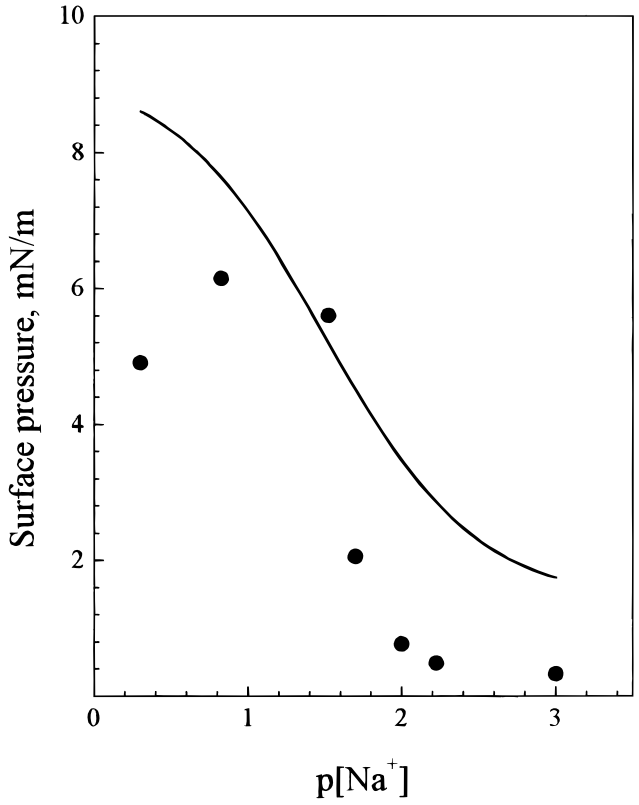

Figure 7. Calculated electrostatic contribution π_{el} to the surface pressure (straight line) compared with the measured π values (●) at a mean area per molecule of 0.85 nm^2.

Conclusions

BAM observations on spread monolayers of DPPG on subphases containing different amounts of NaCl show that inhomogeneities in the monolayers appear after spreading at large mean areas per monolayer molecule and low (lower than 0.15 M NaCl) electrolyte concentration in the subphase. The assumptions that (i) after spreading DPPG is completely hydrolyzed, (ii) dissociation of the resulting acid depends on the electrolyte concentration in the subphase, and (iii) nondissociated acid molecules form solidlike aggregates in the monolayer while the dissociated form represents the surrounding liquid-expanded phase are supported by a detailed analysis of the experimental data. Several parameters of the monolayer have been obtained: degree of aggregation β, dissociation constant in the monolayer K_d^s, and the electrostatic contribution to the surface pressure π_{el}. Satisfactory agreement achieved between π_{el} and the experimentally measured surface pressures supports the reasonability of the calculated value of K_d^s. The described procedure can be recommended for the determination of K_d^s in the case of charged monolayers.

Acknowledgment. This work was carried out with the financial support from the DAAD (A/96/28713, D. Grigoriev), the DFG (Mi 418/7-1 and Pi 165/7-1), and the Dr. A. Kalojanoff Stiftung, München (R. Krustev) at the MPI für Kolloid- und Grenzflächenforschung, Berlin.

References and Notes

(1) Keough K. M. W. In *Pulmonary surfactants*; Robertson, B., van Golde, L. M. G., Batenburg, J. J., Eds.; Elsevier: Amsterdam, 1992.
(2) Zuidam, N. J.; Crommelin, D. J. A. *J. Pharm. Sci.* **1995**, *84*, 1113.
(3) Mota, F. M.; Busquets, M. A.; Reig, F.; Alsina, M. A.; Haro, I. *J. Colloid Interface Sci.* **1997**, *188*, 81.
(4) Mestres, C.; Ortiz, A.; Haro, I.; Reig, F.; Alsina, M. A. *Langmuir* **1997**, *13*, 5669.
(5) Mestres, C.; Alsina, M. A.; Busquets, M. A.; Muranyi, I.; Reig, F. *Int. J. Pharm.* **1998**, *160*, 99.
(6) Jones, M. N.; Song, Y. H.; Kaszuba, M.; Reboiras, M. D. *J. Drug Targeting* **1997**, *5*, 25.
(7) Mestres, C.; Haro, I.; Reig, F.; Alsina, M. A. *Biomed. Chromatogr.* **1997**, *11*, 172.
(8) Perezgil, J.; Casals, C.; Marsh, D. *Biochemistry* **1995**, *34*, 3964.
(9) Williams, A. D.; Wilkin, J. M.; Dluhy, R. A. *Colloid Surf. A* **1995**, *102*, 231.
(10) Taneva, S.; Mceachren, T.; Stewart, J.; Keough, K. M. W. *Biochemistry* **1995**, *34*, 10279.
(11) Taneva, S. G.; Keough, K. M. W. *Biochim. Biophys. Acta* **1995**, *1236*, 185.
(12) Post, A.; Nahmen, A. V.; Schmitt, M.; Ruths, J.; Riegler, H.; Sieber, M.; Galla, H. J. *Mol. Membr. Biol.* **1995**, *12*, 93.
(13) Vonnahmen, A.; Post, A.; Galla, H. J.; Sieber, M. *Eur. Biophys. J.* **1997**, *26*, 359.
(14) Nag, K.; Perezgil, J.; Cruz, A.; Keough, K. M. W. *Biophys. J.* **1996**, *71*, 246.
(15) Vonnahmen, A.; Schenk, M.; Sieber, M.; Amrein, M. *Biophys. J.* **1997**, *72*, 463.
(16) Vonnahmen, A.; Post, A.; Galla, H. J.; Sieber, M. *Eur. Biophys. J.* **1997**, *26*, 359.
(17) Amrein, M.; Vonnahmen, A.; Sieber, M. *Eur. Biophys. J.* **1997**, *26*, 349.
(18) Koppenol, S.; Tsao, F. H. C.; Yu, H.; Zografi, G. *Biochim. Biophys. Acta* **1998**, *1369*, 221.
(19) Helm, C. A.; Laxhuber, L.; Lösche, M.; Möhwald, H. *Colloid Polym. Sci.* **1986**, *264*, 46.
(20) Israelachvili, J. N. *Intermolecular and surface forces*; Academic press: London, 1985; Chapter 12.
(21) Sacre, M. M.; Tocanne, J. F. *Chem. Phys. Lipids* **1977**, *18*, 334.
(22) Hönig, D.; Möbius, D. *J. Phys. Chem.* **1991**, *95*, 4590.
(23) Lösche, M.; Sackmann, E.; Möhwald, H. *Ber. Bunsen-Ges. Phys. Chem.* **1983**, *87*, 848.
(24) Siegel, S.; Vollhardt, D. *Prog. Colloid Polym. Sci.* **1994**, *97*, 16.
(25) Lösche, M.; Duwe, H.-P.; Möhwald, H. *J. Colloid Interface Sci.* **1988**, *126*, 432.
(26) Lakhdar-Ghazal, F.; Tichadou, J.-L.; Tocanne, J. F. *Eur. J. Biochem.* **1983**, *134*, 531.